6. G. P. Cherepanov, Mechanics of Brittle Failure [in Russian], Nauka, Moscow (1974).
7. E. N. Sher, "A case of equilibrium in a radial crack system," Zh. Prikl. Mekh. Tekh. Fiz., No. 5 (1974).
8. R. A. Westman, "Pressurized star crack," J. Math. Phys., 43, No. 3 (1964).
9. V. M. Kuenetsov and A. F. Shatsukevich, "The interaction of detonation products with the laws of the explosion cavity in soils and rocks," Fiz. Goreniya Vzryva, 13, No. 5 (1977).
10. V. M. Komir, V. M. Kuznetsov, and A. F. Shatsukevich, "The effects of gaseous detonation products on the damage to rocks from explosion," FTPRPI, No. 6 (1979).
11. A. P. Bobryakov, G. N. Pokrovskii, and B. N. Serpeninov, "A study of the damage from impact in flat specimens," in: Aspects of Rock Damage Mechanisms [in Russian], IGD Sib. Otd. Akad. Nauk SSSR, Novosibirsk (1976).
12. D. V. Dubnov, N. S. Bakharevich, and A. I. Romanov, Commercial Explosives [in Russian], Nedra, Moscow (1973).

NUMERICAL MODELING OF THE PROCESS OF PENETRATION OF A RIGID BODY OF REVOLUTION INTO AN ELASTOPLASTIC BARRIER

V. I. Kondaurov, I. B. Petrov,
and A. S. Kholodov

UDC 539.3

We will consider the axisymmetric problem of the penetration of an absolutely rigid body of revolution into a deformable barrier of finite thickness. The rheology of the barrier material is described by the equations of flow of elastoplastic bodies. Important aspects of these problems are the sharply expressed wave character of the solution and the large deformations suffered by the barrier. Penetration problems have been the subject of a large number of experimental investigations, which have been used as a basis for studying the effect of various controlling parameters and observable effects and constructing various approximate methods of calculating penetration processes. However, a fully detailed picture of the processes of interaction of projectiles and deformable targets can be obtained only by means of the numerical solution of problems of this kind on the basis of various rheological models and a subsequent comparison with the experimental results in order to refine the mathematical model.

The complex nature of these problems imposes rigid constraints on the choice of a numerical method of solution, the choice of independent variables, etc. In particular, for large penetration depths the use of traditional Lagrangian variables leads to considerable distortions (and often to a loss of regularity) of the difference net and the need to reconstruct it periodically (which may lead to a significant loss of accuracy). The use of fixed Eulerian coordinates leads to difficulties in formulating the boundary conditions at the surface of the barrier and the need to choose a difference net with a large number of nodes in order to obtain acceptable accuracy in a continuous calculation without explicit isolation of the barrier surface. Both these approaches have been used in the numerical solution of problems of this kind, for example, in [1-5]. Here we shall use a moving coordinate system (tied to the upper and lower edges of the barrier) and the net-characteristic method [6], which allows the most natural construction of the computational algorithm near the edges of the region of integration and to a certain extent makes it possible to take into account the region of variation and the wave character of the solution. This explicit scheme of the first order of accuracy is one of those with a positive approximation (monotonic and majorant schemes, to use another terminology) and, as shown in [7], has minimum approximation viscosity among the explicit two-layer schemes of this kind, which is an important property in the continuous calculation of nonsmooth (discontinuous) solutions without explicit isolation of the surfaces of discontinuity [8].

Moscow. Translated from Zhurnal Prikladnoi Mekhaniki i Tekhnicheskoi Fiziki, No. 4, pp. 132-139, July-August, 1984. Original article submitted June 8, 1983.

Formulation of the Problem

In order to describe the behavior of a deformable barrier under the dynamic loads imposed by an absolutely rigid projectile we will use the system of equations [9]

$$\rho\dot{\mathbf{V}} - \operatorname{div}\boldsymbol{\sigma} = 0, \quad \dot{\boldsymbol{\sigma}} - \mathbf{Q}[\nabla\mathbf{V}] = 0, \tag{1}$$

which includes the equations of motion and the Prandtl–Reuss rheological equation for a homogeneous isotropic elastic–perfectly plastic material subject to the Mises yield condition

$$f(\sigma) = \operatorname{tr}(s\cdot s) - 2k^2 = 0, \quad k = \text{const}. \tag{2}$$

In relation (1) the quantity $Q = Q(\sigma)$ is a fourth-order tensor, which in the Eulerian coordinate system x^i with metric tensor g_{ij} for yield condition (2) has the form

$$Q_{ij}^{kl} = \lambda g_{ij}g^{kl} + \mu\left(\delta_i^k\delta_j^l + \delta_j^k\delta_i^l\right) - \frac{\mu}{k^2}H(f)\,s_{ij}s^{kl}. \tag{3}$$

In (1) the dot denotes the material derivative with respect to time t; ρ is the density of the material in the actual configuration of the body; σ is the Cauchy stress tensor; $s = \sigma - (1/3)\operatorname{tr}\sigma\cdot I$ is the stress deviator; I is the unit tensor; k is the yield point in shear; λ, μ are elastic constants; H(f) is a function equal to zero at $f < 0$, and to unity at $f \geqslant 0$.

It can be shown [4] that system (1) is suitable for describing the finite strains of an isothermal elastoplastic medium, if the following constraints hold:

$$\rho_0V_0^2/\sigma_0, \quad \sigma_0/k \sim O(1), \quad (\sigma_0/\mu)^2 \ll 1, \tag{4}$$

where ρ_0, V_0, σ_0 are the characteristic density, velocity, and stress respectively.

Constraints (4) correspond to impact velocities of the order of the plastic wave velocity $[(\lambda + 2\mu/3)/\rho_0]^{1/2}$. In this case the terms associated with the rotation of the particle as a rigid whole in the stress variation rate tensor can be neglected and $\dot{\boldsymbol{\sigma}}$ used instead.

In the approximation considered system of equations (1) in the components $\mathbf{V}$, $\boldsymbol{\sigma}$ is a quasilinear hyperbolic system with four families of characteristic surfaces. The propagation velocities c_i of these surfaces relative to the particles of the medium in the direction of the normal ν are given by the relations [10]

$$\rho c_{1,2}^2 = \mu + \frac{\lambda+\mu}{2}\left(1 - \tilde{\varkappa}^2\mathbf{s}\cdot\mathbf{s}\right)\left\{1 \pm \left(1 + \frac{4\tilde{\varkappa}^2\,|\mathbf{s}+\nu|^2}{1-\tilde{\varkappa}^2\mathbf{s}\cdot\mathbf{s}}\right)^{1/2}\right\},$$
$$c_3^2 = \mu/\rho, \quad c_4^2 = 0, \quad \mathbf{s} = s\cdot\mathbf{v}, \quad \tilde{\varkappa} = \frac{\mu}{\lambda+\mu}\frac{H(f)}{k^2}. \tag{5}$$

For the plane and axisymmetric problems the cone corresponding to c_3 drops out.

In the case of axial symmetry ($x^1 \equiv R$, $x^2 \equiv Z$, $x^3 \equiv \theta$, $\partial/\partial\theta \equiv 0$) and the dimensionless variables $\bar{x}^i = x^i/x_0$, $\bar{V}_R = V_R/V_0$, $\bar{V}_Z = V_Z/V_0$, $\bar{t} = tV_0/x_0$, $V_0 = \sqrt{k/\rho_0}$, $\bar{\sigma}_{RR} = \sigma_{RR}/k$, $\bar{\sigma}_{ZZ} = \sigma_{ZZ}/k$, $\bar{\sigma}_{\theta\theta} = \sigma_{\theta\theta}/k$, $\bar{\sigma}_{RZ} = \sigma_{RZ}/k$, $\bar{\lambda} = \lambda/k$, $\bar{\mu} = \mu/k$, $\bar{\rho} = \rho/\rho_0$, where the velocity and stress components with subscripts R, Z, and θ denote the physical components of the vector $\mathbf{V}$ and the tensor $\boldsymbol{\sigma}$, system (1) is written in the form

$$\frac{\partial\mathbf{u}}{\partial t} + A^k\frac{\partial\mathbf{u}}{\partial x^k} - \mathbf{f} = 0, \quad k = 1,2, \quad \mathbf{u} = \{V_R, V_Z, \sigma_{RR}, \sigma_{ZZ}, \sigma_{\theta\theta}, \sigma_{RZ}\}. \tag{6}$$

The nonzero coefficients of the matrices A^k are as follows:

$$A_{13}^1 = A_{26}^1 = A_{16}^2 = A_{25}^2 = -1, \quad A_{31}^1 = g_1^2 - \lambda - 2\mu,$$
$$A_{32}^1 = A_{61}^1 = A_{31}^2 = g_1g_4, \quad A_{41}^1 = g_1g_3 - \lambda, \quad A_{42}^1 = A_{41}^2 = g_3g_4,$$
$$A_{51}^1 = A_{32}^2 = g_2g_1 - \lambda, \quad A_{52}^1 = A_{51}^1 = A_{62}^2 = g_2g_4,$$
$$A_{62}^1 = A_{61}^2 = g_4^2 - \mu, \quad A_{42}^2 = g_2g_3 - \lambda, \quad A_{52}^2 = g_2^2 - \lambda - 2\mu,$$
$$\mathbf{g} = \{\varkappa s_{RR}, \varkappa s_{\theta\theta}, \varkappa s_{ZZ}, \varkappa s_{RZ}\}, \quad \varkappa^2 = \mu H(f)/k^2,$$
$$\mathbf{f} = \left\{\frac{\sigma_{RR}-\sigma_{\theta\theta}}{\rho R}, \frac{\sigma_{RZ}}{\rho R}, (g_1g_3 - \lambda)\frac{V_R}{R}, \left(g_3^2 - \lambda - 2\mu\right)\frac{V_R}{R}, (g_2g_3 - \lambda)\frac{V_R}{R}, g_3g_4\frac{V_R}{R}\right\}.$$

We will now formulate boundary conditions for system (6) corresponding to the problem of an absolutely rigid circular cylinder with a conical head in axial impact against an elastoplastic barrier occupying at the initial time $t = 0$ the region $\{0 \leqslant R \leqslant R_0, 0 \leqslant Z \leqslant 1\}$, where R_0 is the ratio of the original radius of the barrier to its thickness. Let the lateral (cylindrical) part of the barrier be rigidly fixed, i.e., let the velocities of points on it be equal to zero. We denote by $Z^{H,B} = Z^{H,B}(t, R)$ the functions giving the instantaneous position of the lower and upper edges, which are subject to determination together with $\mathbf{u}(t, R, Z)$.

For the functions $Z^{H,B}(t, R)$ the following equations hold:

$$\left.\frac{\partial Z^{B,H}(t, R)}{\partial t}\right|_R + V_R(t, R, Z^{B,H}(t, R))\frac{\partial Z^{B,H}(t, R)}{\partial R} = V_Z(t, R, Z^{B,H}(t, R)), \tag{7}$$

which make it possible to determine the shape of the surfaces $Z^{B,H}(t, R)$ from their initial shape $Z^B(0, R) = 1$, $Z^H(0, R) = 0$.

Equation (7) follows from the differentiation with respect to t of the dependences $Z^{H,B} = Z^{H,B}[R(\xi^i, t), t]$ as a complex function of time t and the Lagrangian coordinates ξ^i and the definition of the velocity vector of a material particle. We note that the condition $V_R \equiv 0$ at $R = 0$ and $R = R_0$ makes it unnecessary to establish boundary conditions for (7), i.e., the solution of (7) is completely defined by the initial data alone.

The solution of system of equations (6) was determined in the region $\{0 \leqslant R \leqslant R_0, Z^H(t, R) \leqslant Z \leqslant Z^B(t, R)\}$ with the unperturbed initial conditions $\mathbf{u}(0, R, Z) = 0$.

The boundary conditions on the lateral surface of the barrier $R = R_0$, $0 \leqslant Z \leqslant 1$ take the form

$$V_R(t, R_0, Z) = V_Z(Z, R_0, t) = 0.$$

The lower surface of the barrier $Z = Z^H(t, R)$ was taken to be unloaded

$$\sigma_{nn}(t, R, Z^H(t, R)) = \sigma_{nt}(t, R, Z^H(t, R)) = 0. \tag{8}$$

On the upper surface of the barrier, depending on whether for the given values of R, t it is in contact with the surface of the projectile or not, we imposed either conditions (8) or

$$\begin{gathered} V_n = V_B(t)/\sqrt{1 + (\partial Z^B/\partial R)^2},\ \sigma_{nt}(t, R, Z^B(t, R)) = 0, \\ V_n = \left(V_Z - V_R\frac{\partial Z^B(t, R)}{\partial R}\right)\Big/\sqrt{1 + (\partial Z^B/\partial R)^2}, \end{gathered} \tag{9}$$

where $V_B(t)$ 0 is the projectile velocity determined from the equation of motion

$$m_0 dV_B/dt = \int\limits_{S_*} \sigma_{nn} dS, \quad V_B(0) = -V_B^0, \quad dS = 2\pi R dR.$$

Here, the integration is carried out for all values of R for which $Z^y(t, R) \leqslant Z^B(t, R)$ and $\sigma_{nn}(t, R, Z^B(t, R)) < 0$, and m_0 is the mass of the projectile, $Z^y = \psi(t, R) = \psi(0, R) + \int\limits_0^t V_B(\tau)\, d\tau$, $R \leqslant R_0^*$ is the equation of the surface of the head of the axisymmetric projectile (for a conical head $\psi(0, R) = 1 + R\tan\varphi$). If $Z^B(t, R)$, determined from (7), is less than $\psi(t, R)$, then for these values of R we used boundary conditions (8); in the opposite case we assumed $Z^B(t, R) = \psi(t, R)$ and used boundary conditions (9). For those values of R for which at time t the requirement $Z^B(t, R) = \psi(t, R)$ has already been met, we used conditions (9), but if, in this case, $V_n < V_B(t)/\sqrt{1 + (dZ^B/dR)^2}$, then the subsequent computation of $Z^B(t, R)$ was carried out in accordance with (7) and using boundary conditions (8).

On the axis of symmetry $R = 0$ we used the asymptotic equations obtained from (6) by passage to the limit as $R \to 0$. In this case

$$V_R = 0,\ \sigma_{RR} = \sigma_{\theta\theta},\ \sigma_{RZ} = 0,\ R = 0,\ Z^H(t, 0) \leqslant Z \leqslant Z^B(t, 0). \tag{10}$$

For the numerical calculations we used a moving coordinate system $\eta^i = \eta^i(x^m, t)$ such that

$$\eta^1 = R/R_0,\ \eta^2 = (Z - Z^H)/(Z^B - Z^H). \tag{11}$$

Relations (11) map the actual configuration of the body onto the unit square, the uniform coordinate net in the plane (η^1, η^2) corresponding in the plane (R, Z) to a curvilinear net, whose step is constant for fixed R.

If we introduce the notation $\eta^i_m = \partial\eta^i/\partial x^m$, $w^i = \partial x^i/\partial t\big|_{\eta^m}$, then system (6) in the variables (t, η^i) can be written in the form

$$\partial \mathbf{u}/\partial t\big|_{\eta^i} + \mathbf{B}^m(\partial \mathbf{u}/\partial \eta^m) - f = 0,$$

$$\mathbf{B}^m = \eta_i^m\{\mathbf{A}^i - (V^i - w^i)\mathbf{I}\}, \quad 0 \leqslant \eta^i \leqslant 1, \quad i, m = 1, 2, \tag{12}$$

$$R = R_0\eta^1, \ Z = Z^{\text{H}}(\eta^1, t) + \eta^2[Z^{\text{B}}(\eta^1, t) - Z^{\text{H}}(\eta^1, t)].$$

As before system (12) is hyperbolic. The rates $\lambda^\alpha(\alpha = 1, 2, \ldots, 6)$ of propagation of weak discontinuities in the direction of the normal $n_i = \nu_m(\partial x^m/\partial \eta^i)$ are given by the expression

$$\lambda^\alpha = c_\alpha + (V^m - w^m)\,\eta_m^i n_i,$$

where c_α are given by relations (5).

From the hyperbolicity it also follows [11] that there exists a nondegenerate matrix $\omega = \omega(u, n)$ such that

$$\omega_{\alpha\beta}B_{\beta\gamma}^m n_m = \omega_{\alpha\beta}\lambda^\alpha\delta_{\beta\gamma} \quad (m = 1, 2, \ \alpha, \beta, \gamma = 1, 2, \ldots, 6), \tag{13}$$

where there is no summation with respect to α. As may be seen from (13), the rows of ω are the left-hand eigenvectors of the matrix $\mathbf{B}^n n_m$.

We now denote the matrix ω, corresponding to $\mathbf{n} = (1, 0)$ by the symbol ω^1. Multiplying system (12) from the left by ω^1 and using (13), we obtain the characteristic form of the system of equations

$$\omega_{\alpha\beta}^1\left(du_\beta/ds_1^\alpha\right) + \omega_{\alpha\beta}^1 B_{\beta\gamma}^2\left(du_\gamma/d\eta^2\right) = \omega_{\alpha\beta}^1 f_\beta, \tag{14}$$

where there is no summation with respect to α; $du_\beta/ds_1^\alpha = \partial u_\beta/\partial t + \lambda_1^\alpha(\partial u_\beta/\partial \eta^1)$ is the derivative along the bicharacteristic corresponding to the velocity λ_1^α and the normal $\mathbf{n} = (1.\ 0)$. Multiplying (14) from the left by $\Omega^1 = (\omega^1)^{-1}$, we obtain

$$\Omega_{\alpha\beta}^1\omega_{\beta\gamma}^1\left(du_\gamma/ds_1^\beta\right) + B_{\alpha\gamma}^2\left(\partial u_\gamma/\partial \eta_2\right) = f_\alpha. \tag{15}$$

Similarly, denoting by ω^2 the matrix ω for the value $\mathbf{n} = (0, 1)$ and $\Omega^2 = (\omega^2)^{-1}$, we find

$$\Omega_{\alpha\beta}^2\omega_{\beta\gamma}^2\left(du_\gamma/ds_2^\beta\right) + B_{\alpha\gamma}^1\left(\partial u_\gamma/\partial \eta^2\right) = f_\alpha. \tag{16}$$

From (12), (15), and (16) there follows

$$\partial u_\alpha/\partial t\big|_{\eta^m} = \Omega_{\alpha\beta}^m\omega_{\beta\gamma}^m\left(du_\gamma/ds_m^\beta\right) - f_\alpha \ (m = 1, 2, \ \alpha, \beta, \gamma = 1, 2, \ldots, 6). \tag{17}$$

Apart from the derivative with respect to time, equation (17) contains derivatives only along the bicharacteristics and is convenient for constructing the characteristic methods of calculation.

Numerical Calculation Method

For the numerical solution of these boundary-value problems we used the explicit net-characteristic method [6, 7] of continuous computation. In this method the solution is obtained layerwise at t = const, and the nodes of the difference net are formed by the intersection of the lines η^m = const. Each node is defined by the numbers (l_1, l_2, n), where $\eta^i = l_i h_i$, t = 1, 2, where h_i is the step with respect to the space coordinates, $t = \sum_n \tau_n$, τ_n is the step with respect to time. In order to compute the solution vector $\mathbf{u}$ in an inner node on the layer n + 1 from the values of the n-th layer, we use the relations

$$\mathbf{u}_{l_1l_2}^{n+1} = \mathbf{G}\mathbf{u}_{l_1l_2}^n + \tau\mathbf{f}_{l_1l_2}^n, \quad \mathbf{G} = \mathbf{I} + \frac{\tau_n}{h_i}\{\Omega^i\Lambda_+^i\omega^i\Delta_-^i - \Omega^i\Lambda_-^i\omega^i\Delta_+\}_{l_1l_2}^n, \quad \Lambda_+^i = 0{,}5(\Lambda^i + |\Lambda^i|), \quad \Lambda_-^i = 0{,}5(\Lambda^i - |\Lambda^i|), \tag{18}$$

where Λ^i are diagonal matrices composed of eigenvalues λ^α, $\Delta_\pm^i$ are the right-hand and left-hand differences of the solution vector on the n-th layer along the coordinate line η^i.

The difference scheme (18) follows from (17) when the derivatives along the bicharacteristics du/ds_i^β are replaced by the difference relation $(\mathbf{u}_{l_1l_2}^{n+1} - \mathbf{u}_{(\beta,i)})/\tau_n$, where $\mathbf{u}_{(\beta,t)}$ is the value of the solution vector at the point of intersection of the bicharacteristic corresponding to λ_i^β and the coordinate line η^i on the n-th time layer. The value of $\mathbf{u}_{(\beta,k)}$ is obtained from the values of $\mathbf{u}_{l_1l_2}^n$ at the nearest two nodes of the net by linear interpolation. Consequently, the scheme in question has a five-point pattern.

Scheme (18) has the least approximation viscosity among the explicit two-layer schemes of first order of accuracy [6, 7] and belongs to the class of schemes generating a monotonic "smeared" shock wave profile [8].

In order to compute the solution at the boundaries we used the two boundary conditions (9) and four equations in characteristic form that correspond to characteristic planes passing through the body. For the boundary $\eta^1 = 1$ these equations take the form (14), where α = 1, 2, 3, 4, β, γ = 1, 2, ..., 6. Using (13), from which there follows

$$B^2_{\beta\gamma} = \Omega^2_{\beta\alpha}\lambda^{\alpha}_2\omega_{\alpha\gamma},$$

we can write system (14) in the form, analogous to (17), containing only derivatives along the bicharacteristics

$$\omega^1_{\alpha\beta}\frac{du_\beta}{ds^\alpha_1} + \omega^1_{\alpha\beta}\left(\Omega^2_{\beta\gamma}\omega^2_{\gamma\lambda}\frac{du_\lambda}{ds^\gamma_2} - \frac{\partial u_\beta}{\partial t}\right) = \omega^1_{\alpha\beta} f_\beta, \tag{19}$$

α = 1, 2, 3, 4, β, λ, γ = 1, 2, ..., 6; there is no summation with respect to α. As in the case of internal points, in (19) we now replace the derivatives du/ds^α_i by the difference relation $(\mathbf{u}^{n+1}_{l_1 l_2} - \mathbf{u}_{(\beta,i)})/\tau_n$. As a result we obtain a system of four difference equations

$$\boldsymbol{\omega}^1\mathbf{u}^{n+1}_{l_1 l_2} = \tau_n\boldsymbol{\omega}^1\mathbf{f}^n_{l_1 l_2} + \frac{\tau_n}{h_1}\boldsymbol{\Lambda}^1_-\boldsymbol{\omega}^1\Delta_-\mathbf{u}^n_{l_1 l_2} + \frac{\tau}{h_2}\boldsymbol{\omega}^1\left(\boldsymbol{\Omega}^2\boldsymbol{\Lambda}^2_+\boldsymbol{\omega}^2\Delta^2_- - \boldsymbol{\Omega}^2\boldsymbol{\Lambda}^2_-\boldsymbol{\omega}^2\Delta^2_+\right)\mathbf{u}^n_{l_1 l_2},$$

which is closed by two boundary conditions (8), (9).

Results of the Numerical Calculations

In this formulation we calculated the processes of collision of absolutely rigid axisymmetric projectiles with deformable barriers of finite thickness at various values of the parameters defining the problem. Certain results of these calculations are presented in Figs. 1-6.

An important feature of the problem is the strong influence on the solution of the radial unloading waves. There is relatively little concerning this effect in the existing

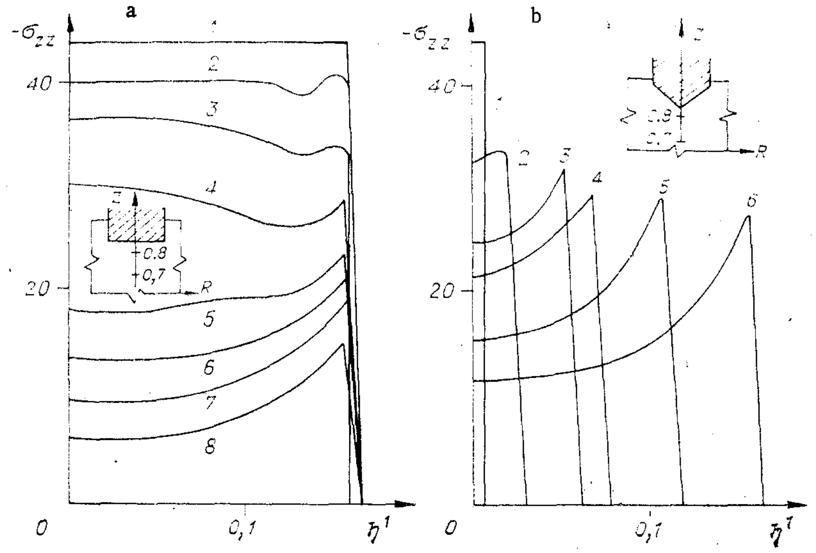

Fig. 1

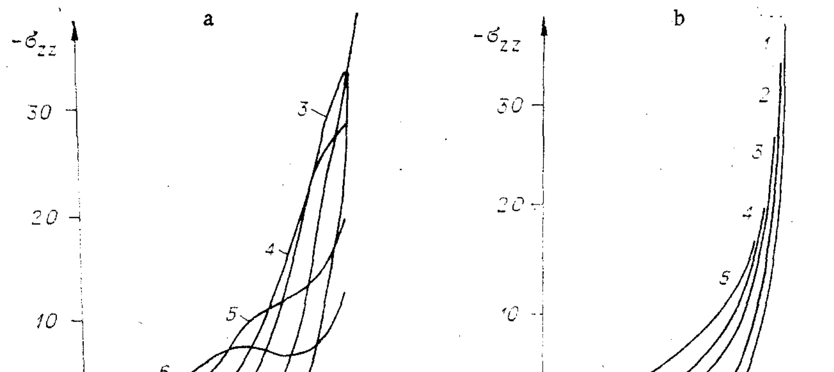

Fig. 2

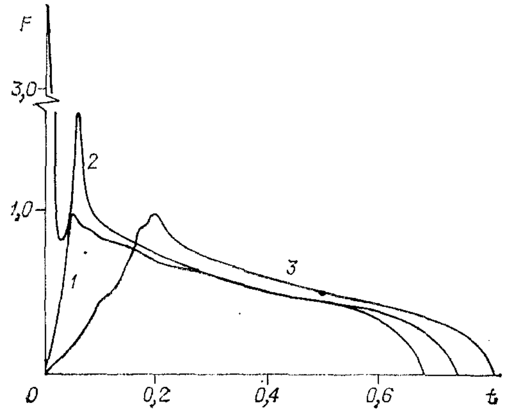

Fig. 3

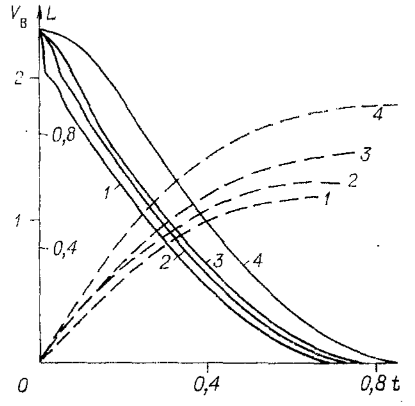

Fig. 4

studies of the penetration of elastoplastic barriers. In particular, as may be seen from the distribution of the stresses $\sigma_{ZZ}(\eta^1)$ at $\eta^2 = 1$ (Fig. 1) and $\sigma_{ZZ}(\eta^2)$ at $\eta^1 = 0$ (Fig. 2), for moments of time at which the perturbations due to the impact of the rigid cylinder and cone have not yet reached the rear face of the barrier, the effect of the radial waves in this initial stage of the penetration process is decisive. In Fig. 1a curves 1-8 correspond to $\varphi = 0.5\pi$, $t = 0$; $3.5\cdot10^{-3}$; $6.43\cdot10^{-3}$; $1.2\cdot10^{-2}$; $1.82\cdot10^{-2}$; $2.1\cdot10^{-2}$; $2.4\cdot10^{-2}$; $3\cdot10^{-2}$; in Fig. 1b the curves 1-6 correspond to $\varphi = 0.25\pi$, $t = 0$; $6.43\cdot10^{-3}$; $2.11\cdot10^{-2}$; $2.7\cdot10^{-2}$; $3.45\cdot10^{-2}$; $6.78\cdot10^{-2}$. In Fig. 2a curves 1-6 correspond to $\varphi = 0.5\pi$, $t = 3.5\cdot10^{-3}$; $6.4\cdot10^{-3}$; $1.2\cdot10^{-2}$; $1.8\cdot10^{-2}$; $2.4\cdot10^{-2}$; $3.0\cdot10^{-2}$; and in Fig. 2b curves 1-5 correspond to $\varphi = 0.25\pi$, $t = 3.5\cdot10^{-3}$; $6.4\cdot10^{-3}$; $1.8\cdot10^{-2}$; $2.4\cdot10^{-2}$; $3.9\cdot10^{-2}$.

Here and in what follows, the calculations were made for the following dimensionless parameters of the problem: $m_0 = 0.174$, $V_B^0 = 2.33$, $R_0^* = 0.16$, $H = 1.0$, $\lambda = 148.0$, $\mu = 99.0$.

The time dependence of the resisting force is represented in Fig. 3. The rapid fall in $F(t) = \int\limits_{S_*} \sigma_{nn} dS$ (S_* is the projection of the contact surface on the plane Z = const) and the presence of a local minimum in the case of a cylindrical projectile (curve 1, $\varphi = 0.5\pi$) indicate the possible "rebound" of the projectile and loss of contact between a sufficiently thin projectile and the thick barrier until the arrival of the tension wave reflected from the rear face ($\eta^2 = 0$), exclusively due to the action of the radial unloading waves. The calculations also show that in the case of a cylindrical projectile the axial symmetry of the problem leads to a considerable increase in the amplitude of the unloading waves converging on the axis R = 0. This may result in the appearance of tensile normal stresses in the neighborhood of the axis R = 0, i.e., "local rebound" of part of the contacting surface, although the resisting force F < 0.

In the case of projectiles with a conical head (curves 2, 3, $\varphi = 0.25\pi$; 0.1π) the F(t) graphs are characterized by an initial increase of F(t) owing to the increase in contact area and the presence of a maximum corresponding to the moment of complete penetration of the head into the barrier. The amplitude of these maxima increases monotonically with increase in the angle φ.

Beyond the maximum (absolute for projectiles with a conical head, local for cylindrical projectiles) the resisting force F decreases to zero. However, its approach to zero is not asymptotic, the derivative dF/dt even increasing at the end of the process. This is because at small loads the barrier behaves elastically, and more rigidly than in the plastic state.

The dependence of the depth of penetration L and the penetration velocity V_B on time t for cylindrical projectiles with a conical head is reproduced in Fig. 4 (dashed and continuous curves respectively). The L(t) curves are monotonic in character, the depth of penetration decreasing with increase in the head half-angle φ. The $V_B(t)$ dependence for cylindrical (curve 1, $\varphi = 0{,}5\pi$) and "blunt" conical projectiles (curve 2, $\varphi = 0.4\pi$) has singularity in the form of a "shelf" or point of inflection corresponding to the same moment of time as the extremum of the F(t) curve in Fig. 3. The presence of this singularity is also due to the radial unloading waves. With decrease in the half-angle of the cone φ (curves 3, 4; $\varphi = 0.25\pi$) this effect disappears. Pointed projectiles are characterized by a slighter fall in the

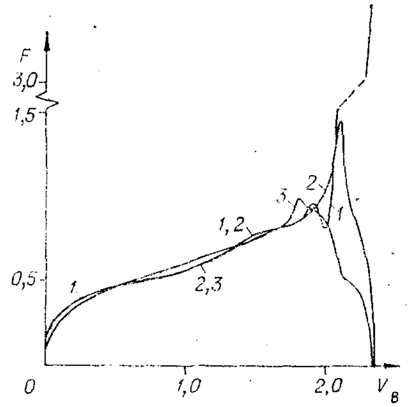

Fig. 5

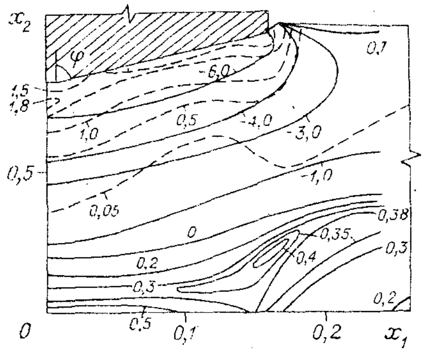

Fig. 6

velocity V_B at the beginning of the process, but subsequently the derivative dV_b/dt is almost the same for any shape of head (the other parameters being equal).

The results obtained indicate that the important influence of the radial stress waves on the penetration process reduces the value of the information obtained by attempting to use plane approximations for calculating the "oblique" nonaxisymmetric collision of a rigid body with a barrier.

The dependence of the force $F = F(V_B)$ on the instantaneous penetration velocity, shown in Fig. 5, is of some interest. Clearly, the calculated family of curves, which depend on the shape of the projectile head, can be divided into two parts: a right-hand part, where there are substantial differences, and a left-hand part, where the curves practically coincide. The boundary between these regions is determined by the position of the extreme right-hand maxima in Fig. 3. Parametrically the dependence of the resisting force on the penetration velocity can be represented in the form

$$F = \begin{cases} F_1(V_B, \chi), & V_B \leqslant V_*(\chi), \\ F_2(V_B), & V_B > V_*(\chi), \end{cases}$$

where χ is the projectile head form parameter (for conical heads the half-angle φ can be taken as χ); V_* is the velocity of the projectile at the moment of total penetration of the sharpest head.

Thus, a difference in the shape of the head affects the $F(V_B)$ dependence only in the initial stage of the axisymmetric process of collision between rigid bodies of revolution and an elastoplastic barrier. This is perfectly consistent with the conclusions of [12], where a similar result was obtained experimentally for cylindrical projectiles with different conical heads, and can be used for creating design-analytical engineering models of penetration processes.

In order to predict the regions of possible failure we calculated the stress energy density fields for plastic strains

$$A_p = \int_t \mathrm{tr}\left(\boldsymbol{\sigma}\cdot\dot{\boldsymbol{\varepsilon}}^p\right) dt = \int_t H(f)\,\mathrm{tr}\,(\mathbf{s}\cdot\nabla\mathbf{V})\,dt$$

and the maximum principal stress fields

$$\sigma_I = \max\left\{\sigma_{\theta\theta},\ 0.5\left[\sigma_{RR} + \sigma_{ZZ} + \sqrt{(\sigma_{RR} - \sigma_{ZZ})^2 + 4\sigma_{RZ}^2}\right]\right\}.$$

In Fig. 6 we have plotted the isolines of A_p and σ_I (dashed and continuous lines, respectively), from which it is clear that a region of shear failure, for which the plastic strain energy A_p constitutes a criterion, is most likely at the tip and edges of the cone. However, failure due to the action of tensile stresses may be localized at the rear face of the barrier following interaction between that face and the compression wave.

In conclusion, we note that a comparison of the results of the calculations for two types of boundary conditions at the cylindrical projectile-barrier contact surface (no slip and slip without friction) revealed a difference of not more than 2% in the value of the penetration depth.

LITERATURE CITED

1. G. P. Men'shikov, V. A. Odintsov, and L. A. Chudov, "Penetration of a cylindrical projectile into a finite plate," Izv. Akad. Nauk SSSR, Mekh. Tverd. Tela, No. 1 (1976).
2. V. A. Gridneva, A. I. Korneev, and V. G. Trushkov, "Numerical method of calculating the state of stress and fracture of a plate of finite thickness subjected to the impact of strikers of various shapes," Izv. Akad. Nauk SSSR, Mekh. Tverd. Tela, No. 1 (1977).
3. V. M. Fomin and N. N. Yanenko, "Numerical modeling of problems of high-velocity interaction," in: Proc. Symp. Nonlinear Deformation Waves, Vol. 2 [in Russian], Tallinin (1978).
4. V. I. Kondaurov and V. N. Kukudjanov, "On constitutive equations and numerical solutions of the multidimensional problems of the dynamics of nonisothermic elastic-plastic media," Arch. Mech., 31, No. 5 (1979).
5. V. M. Fomin and A. I. Gulidov, "Numerical modeling of the rebound of axisymmetric bars from a solid barrier," Zh. Prikl. Mekh. Tekh. Fiz., No. 3 (1980).
6. K. M. Magomedov and A. S. Kholodov, "On the construction of calculation schemes for equations of hyperbolic type on the basis of characteristic relations," Zh. Vychisl. Mat. Mat. Fiz., No. 2 (1969).
7. A. S. Kholodov, "On the construction of difference schemes with a positive approximation for equations of hyperbolic type," Zh. Vychisl. Mat. Mat. Fiz., 18, No. 6 (1978).
8. V. I. Kondaurov and I. V. Roi, "Investigation and use of a conservative difference scheme for the equations of the dynamics of a deformable medium," ChMMSS, 2, No. 2 (1980).
9. L. I. Sedov, Continuum Mechanics, Vol. 2 [in Russian], Nauka, Moscow (1973).
10. V. N. Kukudzhanov and V. I. Kondaurov, "Numerical solution of non-one-dimensional problems of the dynamics of solids," in: Problems of the Dynamics of Elastoplastic Media [Russian translation], Mir, Moscow (1975).
11. R. Courant, Partial Differential Equations [Russian translation], Mir, Moscow (1964).
12. F. F. Vitman and V. A. Stepanov, "Effect of the strain rate on the deformation resistance of metals at impact velocities of 10^2– 10^3 m/sec," in: Some Problems of the Strength of Solids [in Russian], Izd. Akad. Nauk SSSR, Moscow–Leningrad (1959).

MODEL REPRESENTATION OF THE ULTIMATE STRAIN DURING CREEP

M. D. Dacheva, A. M. Lokoshchenko, and S. A. Shesterikov

UDC 539.4:539.376

Within the framework of the Yu. N. Rabotnov conception of the equation of state [1], we consider a description of strain processes under conditions when cumulative damage ω is governing.

We use the version of the equation of state proposed in [2]

$$d\varepsilon/dt = G'(s)ds/dt + F(s); \tag{1}$$

$$d\omega/dt = g'(s)ds/dt + f(s). \tag{2}$$

Equations (1) and (2) determine the change in the total strain ε and the damage ω in the time t up to rupture $t = t^*$. The prime denotes differentiation with respect to the effective stress s. The functions $G'(s)$, $F(s)$, $g'(s)$, and $f(s)$ in (1) and (2) grow monotonically as s increases.

Let a constant tensile force be applied to a specimen and cause a stress σ_0 and a small strain ε. The effective stress in (1) and (2) is a function of the parameter ω. We consider two versions of this function. In the first, we take the dependence

$$s = \sigma_0 \exp \omega, \tag{3}$$

which, for small strain, agrees with the dependence proposed in [3]. In the second version we use the function

$$s = \sigma_0/(1 - \omega), \tag{4}$$

Moscow. Translated from Zhurnal Prikladnoi Mekhaniki i Technicheskoi Fiziki, No. 4, pp. 139-142, July-August, 1984. Original article submitted December 24, 1982.

0021-8944/84/2504-0632$08.50